Microfluid Nanofluid (2010) 8:47–56
DOI 10.1007/s10404-009-0460-3

RESEARCH PAPER

Effects of dynamic contact angle on numerical modeling of electrowetting in parallel plate microchannels

Zahra Keshavarz-Motamed · Lyes Kadem · Ali Dolatabadi

Received: 17 December 2008 / Accepted: 4 May 2009 / Published online: 26 May 2009

Abstract Electrowetting phenomenon in parallel plate microchannel is investigated numerically. The current study advances accuracy of numerical modeling of electrowetting by considering dynamic behavior of the tri-phase contact line using molecular-kinetic theory. This theory in conjunction with volume of fluid method, which has been proved to be a powerful approach for free surface modeling, is used to simulate the phenomenon. By comparing the results against experimental data from literature, the simulation demonstrates significant improvement in results. It is concluded that ignoring dynamic features of wetting leads to overestimation of the effect of electrowetting actuation on various parameters including contact angle, aspect ratio and velocity of the droplet.

Keywords Electrowetting · Molecular-kinetic theory · Dynamic contact angle · Contact line velocity

1 Introduction

Electrowetting on dielectric (EWOD) is the basis of many important microfluidic systems (Mugele and Baret 2005; Erickson 2005). Simplicity of fabrication, low power consumption, rapid switching response and low cost has made it a promising concept for digital microfluidic applications where a tiny amount of liquid in the form of droplets can be manipulated. Besides applications of EWOD in lab-on-a-chip devices (Pollack and Fair 2000; Ren et al. 2002; Pollack et al. 2002; Fouillet et al. 2008), there are several other application fields for EWOD such as micro lenses, fiber optics, display technology and voltage controlled fluidic switches (Mugele and Baret 2005). Electrowetting occurs when a droplet of a conductive liquid is exposed to an external electric field. A change in the electric charge distribution at the liquid/solid interface alters the free energy on the dielectric surface inducing a change in the wettability of the surface and the contact angle of the droplet. Change in the contact angle due to the applied electric potential using the planar capacitor approximation is governed by Young–Lippmann's equation (Adamson 1990; Antropov 2001):

$$\cos\theta = \cos\theta_0 + \frac{C}{2\gamma_{LG}}\psi^2 \tag{1}$$

where θ_0 and θ are contact angles before and after actuation, C the capacitance (per unit area) of the media between the electrode and the liquid, ψ the applied voltage between the liquid and the electrodes and γ_{LG} is the surface tension between the droplet and the surrounding gas.

Contact angle at the tri-phase contact line shows dynamic behavior which plays a crucial role in the movement of liquid droplets on the solid surface but despite its importance, droplet moving studies often ignore this by using a static contact angle. However, for many practical applications, especially at micro level, using this simplification may significantly reduce the accuracy of the simulation. The accurate mechanism of advancing or receding liquid front on a solid surface is not completely understood. As a consequence, prediction of dynamic wetting and dewetting is still complex. One of the well suited approaches to explain the experimental observations and clarify

Z. Keshavarz-Motamed · L. Kadem (✉) · A. Dolatabadi (✉)
Department of Mechanical and Industrial Engineering,
Concordia University, 1515 Ste. Catherine W., Montreal,
QC H3G 2W1, Canada
e-mail: kadem@encs.concordia.ca

A. Dolatabadi
e-mail: dolat@encs.concordia.ca

the underlying physical mechanism is molecular-kinetic theory (Blake 2006). This approach is able to clarify the molecular details of wetting as experimental observations reveal that the contact line motion takes place on a microscopic molecular scale. This theory pictures contact line motion as a series of discrete jumps on the molecular scale involving energy dissipation to overcome the barrier (Blake and Haynes 1969). This approach is based on both molecular and macroscopic scales. Dissipation occurs at the molecular level and its effects can be reflected on the macroscopic level.

As Blake (2006) explained in a recent article, current models of dynamic wetting can be categorized into (a) hydrodynamic models which are based on empirical relations, (b) molecular-kinetic theory and (c) Shikhmurzaev (1993) model. In our numerical simulations, we applied the molecular-kinetic theory, described in the following section, to model dynamic contact angle. As noted by Van Mourik et al. (2005), the empirical models are valid only for positive contact line velocity, i.e. advancing contact line, while Blake's theory is appropriate for both advancing and receding contact lines.

Attempts have been made from various scientific perspectives to obtain theoretical understanding of the dynamic contact angle. Van Mourik et al. (2005) studied several theories about dynamic contact angle applied to volume of fluid (VOF) model and compared the results with experiments. They concluded that in comparison with hydrodynamic based models, molecular-kinetic theory is the best and a highly accurate approach for modeling the phenomenon in conjunction with the VOF technique. Blake et al. (2000) broadened the molecular-kinetic theory to comprise electrostatic effects as well. Other researchers incorporated this model in their experimental studies of dynamic effects of electrowetting (Ren et al. 2002; Wang and Jones 2005; Chen and Hsieh 2006; Decamps and De Coninck 2000).

Understanding dynamics of EWOD is of paramount importance in precise prediction of the performance of droplet based devices. Developing a numerical tool able to accurately simulate electro-hydrodynamic of wetting phenomenon helps designing and manufacturing of lab-on-a-chip devices based on digital microfluidics where conducting experiments at such small scales is complex and costly. Numerous studies showed effectiveness of the VOF method in capturing droplet movement on a solid surface (Hirt and Nichols 1981; Bussmann et al. 1999; Blake 1993; Karl et al. 1996; Fukai et al. 1993). In this study, to investigate droplet actuation under electrowetting forces, numerical simulation based on VOF method (Hirt and Nichols 1981) considering dynamic wetting within the frame of molecular-kinetic theory was performed.

Numerical simulation of electrowetting phenomenon between parallel plates using the VOF method has been reported by Arzpeyma et al. (2008). In that study, contact angle was considered to be static by neglecting dynamic behavior of the tri-phase contact line. The present study is aimed at improving this model by introducing a dynamic contact angle model employing molecular-kinetic theory suggested by Blake (2006).

A brief introduction of molecular-kinetic theory will be followed by an explanation of the numerical methodology. The latter includes a summary of governing equations and free surface tracking method, strategies to integrate dynamic contact angle based on molecular-kinetic theory in the numerical procedure, a description of the geometry and incorporated boundary conditions. In the results and discussion section, effect of applying dynamic contact angle model in the numerical methodology is studied by comparing results of this model against results calculated by static contact angle model in terms of contact angle, droplet deformation and droplet velocity.

2 Molecular-kinetic theory

Molecular-kinetic theory developed by Blake and Haynes (1969) originates from the Frenkel/Eyring view of liquid transport (Glasstone et al. 1941). This theory rejects dissipation due to the viscous flow and states that the energy dissipation occurs at the moving contact line due to the jumping of molecules (attachment or detachment of fluid particles) along the solid surface. Dynamic of wetting is described quantitatively by the velocity at which the liquid moves across the solid and the dynamic contact angle which is the angle formed between the moving liquid interface and the target surface in the vicinity of the contact line. The contact angle of a moving droplet differs from its static value at equilibrium and may be referred to either an advancing or a receding contact angle. Advancing contact angle is an angle that the liquid exhibits in dynamic advancing (wetting) which is larger than equilibrium contact angle while receding angle occurs in dewetting when contact angle is smaller than equilibrium contact angle (Blake 1993; Dussan 1979). It is important to point out that the contact line motion is influenced by both magnitude and direction of the velocity.

In this theory, velocity of the contact line is determined by κ^0 and λ which are the equilibrium frequency of the random molecular displacements and the average length of each displacement, respectively. These displacements occur at the adsorption sites on the solid surface during dissipative and thermodynamically irreversible processes. The out of balance surface tension due to disturbance of

equilibrium (F_W) can drive bulk flow to move the contact line as shown by Eq. 2.

$$F_W = \gamma_{LG}(\cos\theta_S - \cos\theta_D) \tag{2}$$

where θ_S and θ_D are static and dynamic contact angles, respectively. Combining this idea with Frenkel–Eyring activated rate theory of transport in liquids leads the following relationship introduced by Blake (2006) and Blake and Haynes (1969),

$$U = 2\kappa^0\lambda\sinh[\gamma_{LG}(\cos\theta_S - \cos\theta_D)\lambda^2/2k_BT] \tag{3}$$

U, k_B and T are velocity of the contact line, the Boltzmann constant and absolute temperature, respectively. Several expressions for κ^0 based on thermodynamic arguments have been proposed to date. If the argument of sinh function is adequately small, velocity of the contact line can be determined as:

$$\begin{aligned} U &\approx \kappa^0\lambda^3\gamma_{LG}(\cos\theta_S - \cos\theta_D)/k_BT \\ &= \gamma_{LG}(\cos\theta_S - \cos\theta_D)/\xi \end{aligned} \tag{4}$$

where $\xi = k_BT/\kappa^0\lambda^3$ in Eq. 4 is the coefficient of wetting line friction. κ^0 and λ or ξ are determined experimentally. Experimental studies by Ren et al. (2002), Wang and Jones (2005), Chen and Hsieh (2006), Decamps and De Coninck (2000), showed that assumption of small argument for sinh is a valid assumption for the case under investigation.

3 Numerical methodology

3.1 Governing equations

The flow is modeled as incompressible, laminar, three-dimensional and Newtonian flow. Mass conservation and Navier–Stokes equations for this flow can be written as:

$$\nabla\cdot\vec{V} = 0 \tag{5}$$

$$\frac{\partial\vec{V}}{\partial t} + (\vec{V}\cdot\nabla)\vec{V} = -\frac{1}{\rho}\nabla P + \nu\nabla^2\vec{V} + \frac{1}{\rho}\vec{F}_b \tag{6}$$

where $\vec{V}, P, \rho, \nu$ and $\vec{F}_b$ are velocity vector, pressure, liquid constant density, constant liquid viscosity and any body force per unit volume, respectively. This study uses a modified version of the VOF method developed by Bussmann et al. (1999). In this method volume tracking is done by introducing a scalar field f which identifies the volume fraction of the computational cell filled by liquid. Cells with f value between zero and one are interfacial cells while those with f value of zero or unity indicate completely empty or full cells. Solving of the advection equation of volume fraction gives the f field as follow,

$$\frac{\partial f}{\partial t} + (\vec{V}\cdot\nabla)f = 0 \tag{7}$$

Volume tracking algorithm consists of two steps: approximate construction of interface and advection of it. In three dimensions, the interface is reconstructed by locating a plane within each interfacial cell utilizing volume fraction of the cell, f, and normal vector to the interface $\hat{n}$. The reconstructed interface and new velocities are then used to compute volume flux across each cell face in one coordinate direction at a time. Intermediate volume fraction values and interface shape are determined and after advection of the interface in all directions, final volume fraction field and interface shape of that time step are specified.

Instead of considering the surface tension as a pressure jump boundary condition across the interface, its body force equivalent $\vec{F}_{ST}$ is employed, based on the continuum surface force (CSF) model of Brackbill et al. (1992):

$$\vec{F}_{ST}(\vec{x}) = \gamma_{LG}\int_S \kappa(\vec{y})\hat{n}(\vec{y})\delta(\vec{x}-\vec{y})\mathrm{d}S \tag{8}$$

Here integration is done over some area of free surface S, κ is the local total curvature and $\hat{n}$ is the unit normal to the interface, calculated using Eq. 9.

$$\hat{n} = \frac{\nabla f}{|\nabla f|} \tag{9}$$

Geometrical features κ and $\hat{n}$ are related to each other by:

$$\kappa = -\nabla\cdot\hat{n} \tag{10}$$

Surface tension should impose same acceleration on fluids on either side of the interface. By convolving the surface tension force onto fluid in the vicinity of the surface, δ Dirac delta function in Eq. 8 satisfies this requirement. Dynamic or static contact angle is imposed as boundary condition reorienting $\hat{n}$ at nodes on the solid surface. Body force form of the surface tension $\vec{F}_{ST}$ calculated with this strategy is integrated to the Navier–Stokes equations as a part of body force term $\vec{F}_b$. A more detailed description about treatment of CSF can be found in Bussmann et al. (1999).

To calculate electric potential throughout the fluid domain, second order discretized form of the Laplace equation is solved at the beginning of each time step iteratively.

$$\nabla^2\psi(x,y,z) = 0 \tag{11}$$

Equations 5, 6, 7 and 11 are solved on a uniform Cartesian mesh using finite difference method. The numerical algorithm to advance the solution by one time step is depicted in Fig. 1.

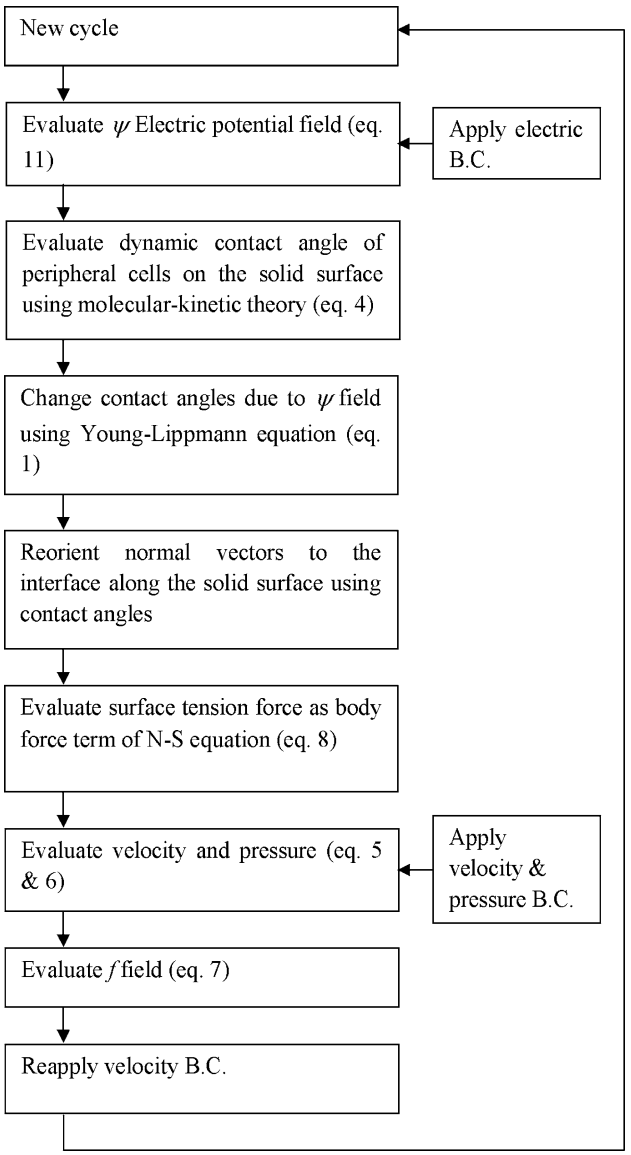

Fig. 1 The algorithm to advance the solution by one time step

3.2 Implementation of dynamic contact angle model

This work uses Eq. 4 in Sect. 2 to introduce dynamic effects of the contact line motion on the droplet movement. Explicitly, free surface tracking numerical methods should solve stress singularity problem by introducing slip boundary condition on the contact line (Fukai et al. 1995). On the contrary, as pointed out by Bussmann et al. (1999), in VOF method since the interface is not tracked explicitly and information about velocities exist at cell faces and not on the interface, a good estimation of the contact line velocity could be considered as the nearest calculated velocity. In this work, we followed their suggestion and considered the normal component of the velocity to the free surface, one half cell height above the solid surface as the tri-phase contact line velocity. Once tri-phase contact line velocity is calculated, contact angle is computed using molecular-kinetic theory to reflect the dynamic features. The calculated dynamic contact angle is then used in the Young–Lippmann's equation and a new contact angle, taking into account both dynamic and electrical effects, is specified and solution continues.

Contact angle considered in this work is macroscopic one and dynamic calculation uses the contact line velocity in its macroscopic sense as the contact angle at the microscopic location of the contact line is not affected by the electric field. Adamiak (2006) nicely summarized concerns regarding contact line and necessity of considering macroscopic contact angle far enough from it. Since treatment of the interface is so that it captures approximate location of the contact line as described in Sect. 3.1, it satisfies the requirement of considering contact angle far from the microscopic location of the contact line.

For closing description of the methodology two further issues should be discussed. First, the calculation procedure assumes that electrical and dynamic effects can be considered independently and the total effect could be studied by superimposing these two effects. Blake et al. (2000) extended molecular-kinetic theory to include electrical effects in this model. They assumed that dynamic wetting and electrostatic effects can be treated independently and presented experimental evidences that the combined model can successfully predict the electrowetting phenomenon. Secondly, in electrowetting driven lab-on-a-chips, favorable surfaces are hydrophobic ones. Calculation of contact angle based on molecular-kinetic theory using rightmost expression of Eq. 4 depends on the friction factor of the surface under investigation. Fortunately, recently few studies reported this value experimentally for hydrophobic materials (Decamps and De Coninck 2000; Ren et al. 2002).

3.3 Geometry and boundary conditions

With the aim of comparison with data of Pollack (2001), this work uses similar geometry and boundary conditions used in their study. A droplet of diameter of 1.9 mm, whose center is located at 1.2 mm from the beginning of the channel positioned by adjusting the volume fraction field (see Fig. 2) is actuated in a parallel plate channel with a length of 10 mm by square electrodes with a length of 1.5 mm and a voltage of 50 V. The water droplet has a volume of 900 nl with a liquid–gas surface tension of 0.0728 N/m and ions from salt which make it conductive. The channel is shaped by two parallel surfaces with a 300 μm gap and coated with Teflon AF 1600 with the static contact angle of 104°. A layer of Parylene C insulator with thickness of 900 nm and three times permittivity of free space is used between electrodes and Teflon layer. The

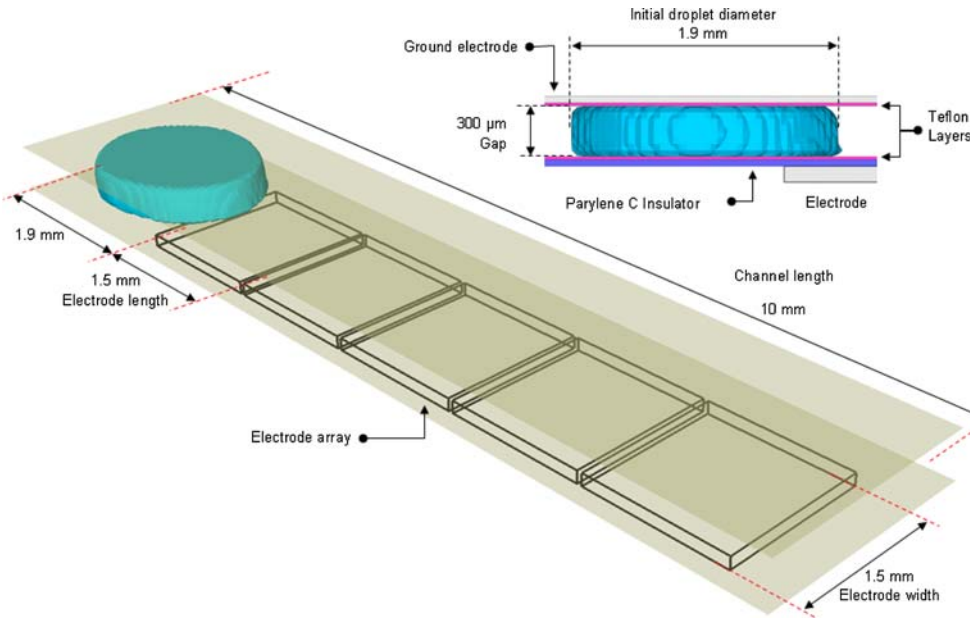

Fig. 2 Schematic diagram of the computational domain

contact line friction factor is considered to be 0.04 Pa s for Teflon AF 1600 as reported by Ren et al. (2002). The droplet inside the parallel plates channel faces an array of the electrodes on the floor and a grounded electrode on the ceiling. Potential of the top electrode is zero and the Teflon layer on it is so thin that the droplet can be assumed to be in contact with this electrode. The applied voltage of the bottom electrodes is applied as the boundary condition to the electric potential equation (Eq. 11). Electric field calculation is done neither inside Teflon layers nor inside insulator layer. The first bottom electrode is located at 1.9 mm from the entrance of the channel. Four other electrodes with no horizontal gap in between are considered after the first one on the floor plate. Electrical facility in channel is, therefore, accessible from 1.9 to 9.4 mm.

The droplet is a conductive solution in contact with the top electrode. Electric potential inside the droplet is considered to be zero. Therefore, electric field calculation is solely done over the air region outlined by the volume fraction field. The electric field influences the droplet movement by changing the droplet's contact angle in the vicinity of tri-phase contact line as described with Eq. 1. The changed contact angle due to electric potential changes the surface tension forces in the Navier–Stokes equations leading to droplet movement. In our simulations, Bond number is very small (0.012). Consequently, we neglected gravity in comparison to the surface tension as the sole constituent of body force term in Navier–Stokes equations. No-slip, no-penetration and zero pressure gradient boundary conditions are applied on the solid surfaces. At the free surface shear stress is considered to be zero and since the surface tension force has already been included in the body force term of the Navier–Stokes equations, zero pressure boundary condition is imposed there.

Boundary condition for electrical actuation is so that only one electrode is on at any time. At the beginning, the droplet is located with zero initial velocity above the first electrode which is on. Once the droplet reaches the next electrode, it is switched on and the former one is turned off by setting its potential to zero and solution continues by passing the droplet above electrodes. Movement of the droplet changes the electric field inside the channel, as electrodes are turned on and off and the droplet's shape with zero potential affects it.

The computational domain was discretized into Cartesian cubic elements of side of 25 and 50 μm in both static and dynamic contact models. Simulations done with these two mesh sizes did not show significant improvement in favor of the finer mesh in calculated velocity for different voltages from 45 to 60 V. Hence, to speed up the calculations, a mesh size of 50 μm was used in the simulations presented in this study. In order to make simulations faster, problem symmetry was taken into consideration and only half the width of the parallel plate channel and droplet were modeled (Fig. 3).

4 Results and discussions

This section discusses differences between results calculated by dynamic and static models in terms of various parameters. Figure 3 gives a gross view of the moving droplet between the parallel plates as being considered in this study. It exhibits electric potential distribution around and in front of the droplet where the electrode under the droplet causes the electrowetting phenomenon by inducing electric field inside the flow domain. It should be noted that

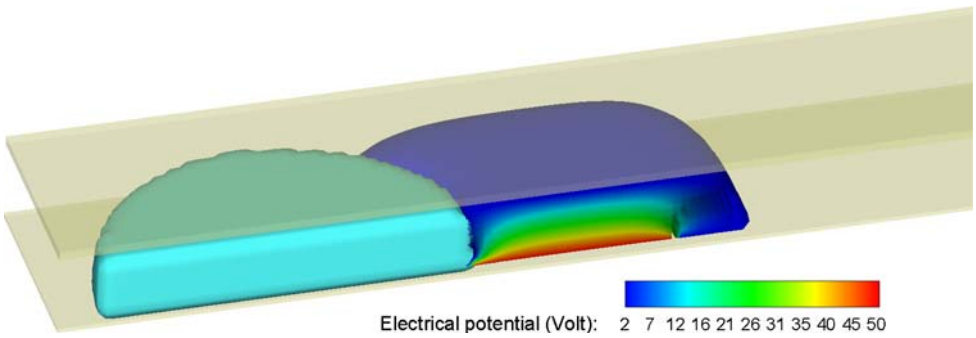

Fig. 3 Electric potential distribution around a moving droplet

everywhere in this paper the actuation voltage is 50 V unless other voltages are stated.

4.1 Droplet contact angle

Contact angle depends on the velocity, as well as other flow field parameters near the wetting line. Therefore, in this study, Eqs. 1 and 4 were solved simultaneously with Eqs. 5–7 and 11 which govern the flow dynamics to take dynamic contact angle into account. Calculated dynamic contact angle for each cell on tri-phase contact line enters to the Young–Lippmann equation to compute the electrically altered contact angle. With the above mentioned strategy, the output of the Young–Lippmann equation in the dynamic model has effects on both hydrodynamic and electrical wetting of the contact line.

Variation of the numerically calculated dynamic contact angles at leading and trailing edges of the droplet using molecular-kinetic theory is illustrated in Fig. 4 and is compared to the static contact angles along the channel. Electrowetting is induced by changing the interfacial energy between the solid and the liquid which leads to a reduction of contact angle to enhance the wettability on the surface. In the static contact angle simulation, when the droplet approaches the electrode and advances on its path, contact angle decreases at the leading edge from 104° to 62° while its trailing edge contact angle stays constant at 104° (Fig. 4). This creates a net force which leads to the movement of the droplet on the electrode path.

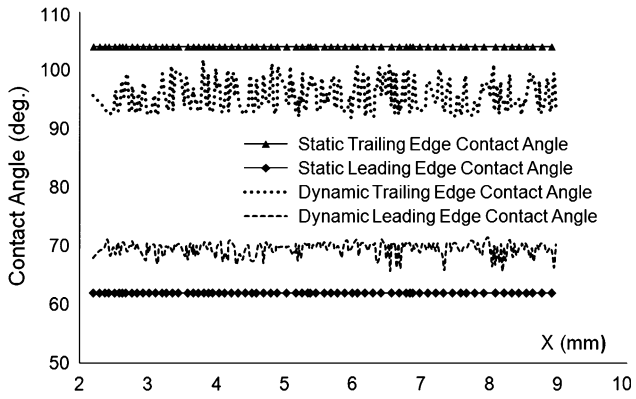

Fig. 4 Computed contact angles actuated by 50 V. In dynamic model the values bear both hydrodynamic and electrical wetting effects

By considering dynamic characteristics of the contact line, animated evolution of the contact angle which is ignored in the static model (Fig. 4) comes into action. The computed leading edge dynamic contact angle is undulating between 67° and 70° and the trailing edge one is altering in the range of 94°–100°. These changing values reflect remarkable effect of the tri-phase contact line velocity on the contact angle which is not accessible in the static model of the contact line.

Figure 5 shows the range of the contact angle occurring in the dynamic simulations in comparison with the static ones. A contact angle of 104°, as shown at the trailing side of the droplet in Fig. 5a, is the static contact angle of the Teflon surface in absence of the electrical actuation. This angle is changed to 62°, when the droplet is affected by the electric potential as seen at the leading edge of the droplet, in Fig. 5a. This electrowetting effect is combined with the dynamic effect of the contact line movement at the leading edge of the droplet in Fig. 5b. By considering the contact line friction, the dynamic model changes the leading and trailing contact angle to a range of 67°–70° and 94°–100°, respectively, for different locations and velocities of the contact line along the channel. Thus, in comparison with the static simulation, the leading edge contact angle is increased by 8° while its trailing edge is decreased by 8°. This phenomenon leads to a decrease in the net force acting on the droplet in the real dynamic situation which results in difference of the droplet movement predicted by two models as discussed below in the velocity section.

3D simulations provide contact angle distribution on the tri-phase contact line as illustrated in Fig. 6 for static and dynamic contact angle models. This figure shows another view of the information, provided in Fig. 5, when the droplet reaches to the third electrode which is featured with an almost steady motion as calculated by the dynamic model (elaborated in Sect. 4.3).

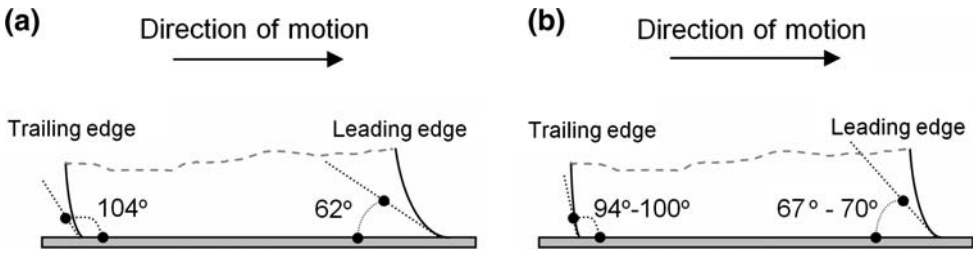

Fig. 5 Schematic presentation of droplet contact angle on Teflon surface, actuated by 50 V. **a** Static, **b** dynamic

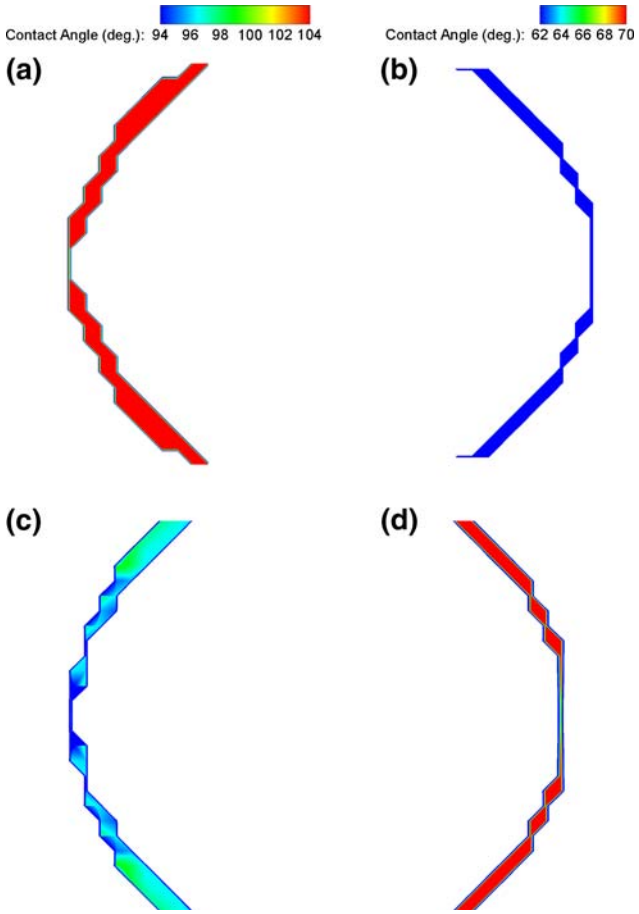

Fig. 6 Schematic presentation of droplet contact angle on Teflon surface, actuated by 50 V. **a** Static trailing edge, **b** static leading edge, **c** dynamic trailing edge, **d** dynamic leading edge

4.2 Droplet deformation

In electrowetting, the applied electric potential on the droplet causes droplet stretching resulting in its movement. Thus, the stretching level of the droplet gives important information about its situation inside the channel. Figure 7 demonstrates that the static simulation overestimates the level of deformation of the droplet in comparison with the dynamic one.

Figure 8 shows how droplet's aspect ratio evolves inside the channel. In this study, aspect ratio is defined as the ratio of droplet length in the direction of motion to the droplet width perpendicular to the direction of motion. This figure demonstrates that considering dynamic characteristic leads to a reduced aspect ratio up to 39% when it reaches to almost steady motion after reaching the third electrode (i.e. $x = 6.4$ mm) as will be explained in Sect. 4.3.

Figure 9 strengthens the argument stated for Figs. 7 and 8 by showing how droplet aspect ratio depends on actuation voltages. In this figure, largest calculated aspect ratio of droplet in the channel is used as a measure of droplet deformation. The dependence of the aspect ratio on voltage demonstrates consistent overestimation of the static model for various voltages.

4.3 Droplet velocity

In molecular-kinetic model, molecular interactions between the liquid and the surface is taken into account by relating the motion of the contact line on the adsorption of molecules on the surface (Blake 2006). Adsorption of liquid molecules is a dissipative process in which their immobilization occurs to some level. Hence, these interactions are the main barrier to the motion of the wetting line. In this study, numerical simulations using molecular-kinetic theory in comparison with the static ones demonstrate inevitable hindrance to the movement of the wetting line.

Droplet's leading edge velocity as computed by two static and dynamic contact angle approaches is compared in Fig. 10. Static model shows faster movement during course of traveling in the channel while by considering molecular level adsorption and dissipation, dynamic model calculates slower movement in the channel. In the onset of motion, since velocity of the contact line is zero, dynamic model predicts similar values as static model. When contact line velocity comes into action, velocity decreases in the dynamic model and becomes almost steady afterward. Conversely, static model calculated increasing velocity for the droplet. When the droplet passes over the third electrode and reaches to quasi-steady motion as modeled by the dynamic model, leading edge velocity of the static model is about five times that of the dynamic one.

Figure 11 strengthen the points mentioned above by showing the droplet location in the parallel plate channel at three different instants of its movement. During the time

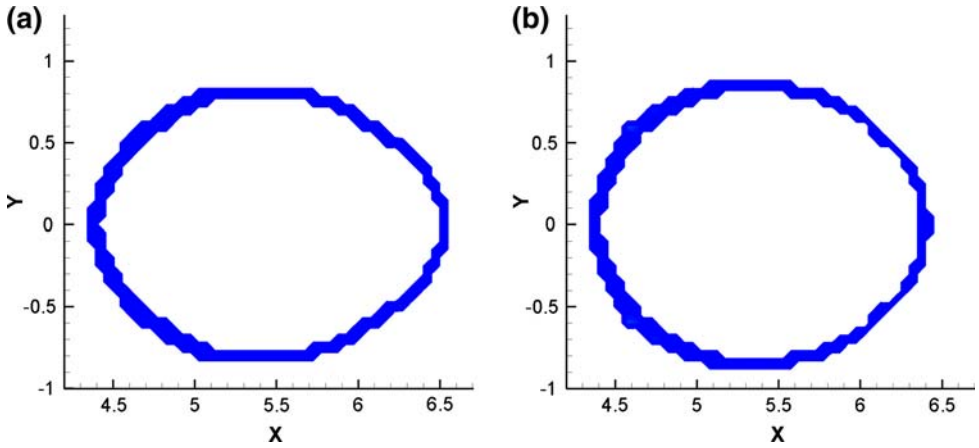

Fig. 7 Droplet deformation **a** static model, **b** dynamic model

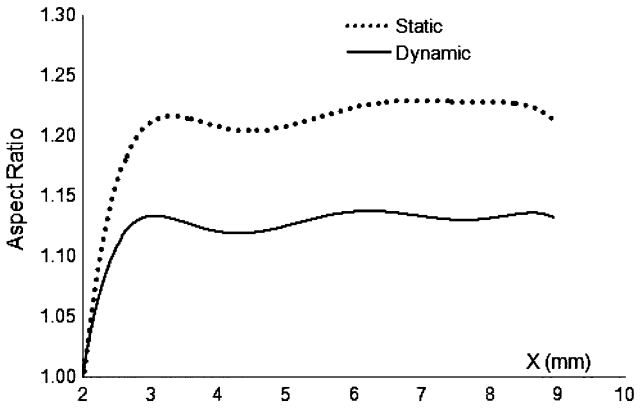

Fig. 8 Aspect ratio of the droplet along parallel plate channel actuated by 50 V

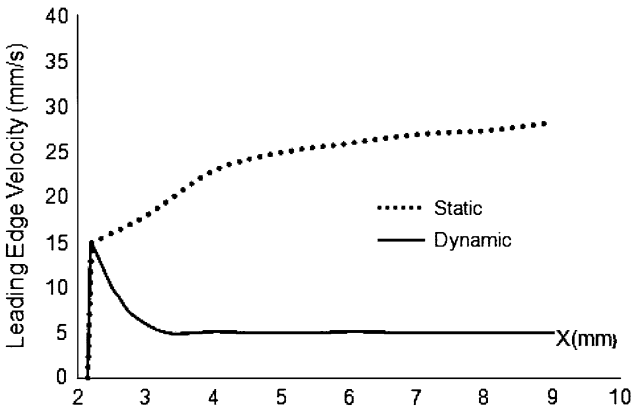

Fig. 10 Comparison of droplet's leading edge velocity in the parallel plate channel between static and dynamic models actuated by 50 V

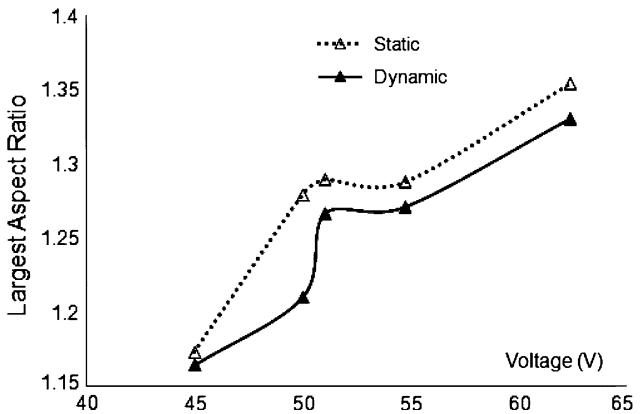

Fig. 9 Largest aspect ratio of the droplet as a function of actuation voltage

required for the droplet to reach almost the end of the channel in the static simulation, it remains in the beginning segment of the channel in the dynamic simulation.

Results of simulating the electrowetting for various actuation voltages for both dynamic and static treatments of the contact angle are compared with experimental results in a study conducted by Pollack (2001) (Fig. 12). Here droplet velocity is defined as average leading edge velocity during motion of the droplet inside the parallel plate channel. This figure illustrates significant improvement of the dynamic model using molecular-kinetic method. In addition, the trend of graph for dynamic case is very close to experimental results by Pollack (2001). It should be noted that, in agreement with Figs. 10 and 11, this figure shows that ignoring dynamic feature of the contact line in simulations leads to an overestimation of droplet velocity for different voltages.

5 Conclusion

Several experimental studies verified validity of molecular-kinetic model for electrowetting applications (Ren et al. 2002; Wang and Jones 2005; Chen and Hsieh 2006; Blake et al. 2000; Decamps and De Coninck 2000) and usability of this model in combination with VOF method in simulating free surface flows (Van Mourik et al. (2005)). In line with those, this study advanced our understanding of electrowetting phenomenon in parallel plate channels

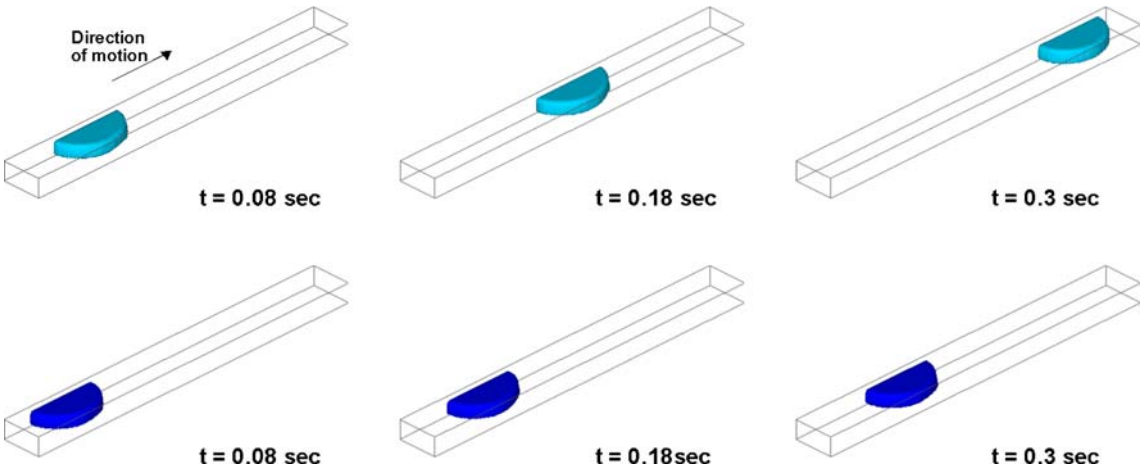

Fig. 11 Comparison of the droplet traveling in static model (*first row*) and dynamic model (*second row*)

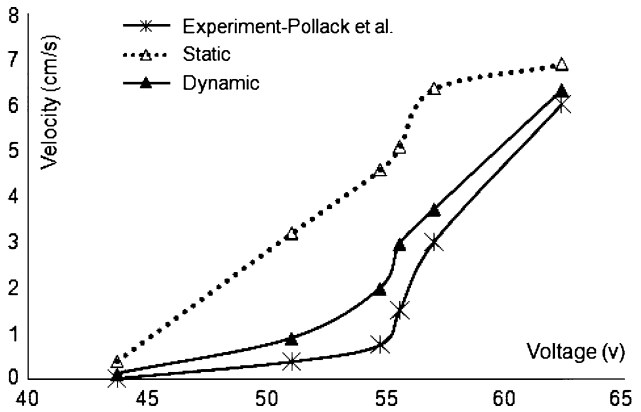

Fig. 12 Comparison of droplet velocity as a function of voltage from dynamic and static model and experiment by Pollack (2001)

considering dynamic effects of moving contact line. Present work showed that ignoring dynamic characteristics of wetting in microscale leads to an overestimation of the effect of electrical actuation on various parameters including contact angle, aspect ratio and velocity of the droplet. Leading edge contact angle predicted by dynamic model is larger than what is calculated by the static model while trailing edge contact angle is smaller than the static one. Study of droplet aspect ratio showed larger values in the static simulation. In addition, we demonstrated that this overestimation in the aspect ratio is consistently present for different voltages. In terms of velocity for various actuation voltages during the course of the movement in the microchannel, static model predicts faster movement in comparison with the dynamic model. The good agreement between experimental and computational results demonstrates significant improvement in numerical predictions by integrating molecular-kinetic theory as the dynamic contact angle model in the numerical methodology.

Acknowledgments The authors would like to acknowledge SIMULENT Inc., Toronto, Ontario for making SIMULENT code accessible for this study. We thank four anonymous reviewers and Nima Maftoon for their many helpful comments. A. D. would like to thank the support of MDEIE and FQRNT.

References

Adamiak K (2006) Capillary and electrostatic limitations to the contact angle in electrowetting-on-dielectric. J Microfluid Nanofluid 2:471–480

Adamson AW (1990) Physical chemistry of surfaces, 5th edn. Wiley, New York

Antropov L (2001) Theoretical electrochemistry. University Press of the Pacific, Honolulu

Arzpeyma A, Bhaseen S, Dolatabadi A, Wood-Adams P (2008) A coupled electro-hydrodynamic numerical modeling of droplet actuation by electrowetting. J Colloids Surf A Physicochem Eng Asp 323:28–35

Blake TD (1993) Dynamic contact angles and wetting kinetics. In: Berg JC (ed) Wettability. Marcel Dekker, New York, pp 251–309

Blake TD (2006) The physics of moving wetting lines. J Colloid Interface Sci 299:1–13

Blake TD, Haynes JM (1969) Kinetics of liquid/liquid displacement. J Colloid Interface Sci 30:421–423

Blake TD, Clarke A, Stattersfield EH (2000) An investigation of electrostatic assist dynamic contact wetting. Langmuir 16:2928–2935

Brackbill JU, Kothe DB, Zemach C (1992) A continuum method for modeling surface tension. J Comput Phys 100:335–354

Bussmann M, Mostaghimi J, Chandra S (1999) On a three-dimensional volume tracking model of droplet impact. J Phys Fluids 11:1406–1417

Chen JH, Hsieh WH (2006) Electrowetting-induced capillary flow in a parallel-plate channel. J Colloid Interface Sci 296:276–283

Decamps C, De Coninck J (2000) Dynamics of spontaneous spreading under electrowetting conditions. Langmuir 16:10150–10153

Dussan VEB (1979) On the spreading of liquids in solid surfaces: static and dynamic contact lines. Annu Rev Fluid Mech 11:371–400

Erickson D (2005) Towards numerical prototyping of labs-on-chip: modeling for integrated microfluidic devices. J Microfluid Nanofluid 4:159–165

Fouillet Y, Jary D, Chabrol C, Claustre P, Peponnet C (2008) Digital microfluidic design and optimization of classic and new fluidic functions for lab on a chip systems. J Microfluid Nanofluid 4:159–165

Fukai J, Zhao Z, Poulikakos D, Megaridis CM, Miyatake O (1993) Modeling of deformation of a liquid droplet impinging upon a flat surface. J Phys Fluids A 5:2588–2599

Fukai J, Shiiba Y, Yamamoto T, Miyatake O, Poulikakos D, Megardis CM, Zhao Z (1995) Wetting effects on the spreading of a liquid droplet colliding with a flat surface experiment and modeling. J Phys Fluids 7:236–247

Glasstone S, Laidler KJ, Eyring HJ (1941) The theory of rate processes. McGraw-Hill, New York

Hirt CW, Nichols BD (1981) Volume of fluid (VOF) method for the dynamic of free boundaries. J Comput Phys 39:201–225

Karl A, Rieber M, Shelkle M, Andres K, Frohn A (1996) Comparison of new numerical results for droplet wall interactions with experimental results. Proc ASME Fluid Eng Div Summer Meet 1:202–206

Mugele F, Baret J (2005) Electrowetting from basics to applications. Top Rev J Phys 17:705–774

Pollack M (2001) Electrowetting-based microactuation of droplets for digital microfluidics. PhD thesis, Duke University, Durham

Pollack MG, Fair RB (2000) Electrowetting-based actuation of liquid droplets for microfluidic applications. J Appl Phys Lett 77:1725–1726

Pollack MG, Shenderov AD, Fair RB (2002) Electrowetting-based actuation of droplets for integrated microfluidic. J Lab Chip 2:96–101

Ren H, Fair RB, Pollack MG, Shaughnessy EJ (2002) Dynamics of electro-wetting droplet transport. J Sens Actuators B 87:201–206

Shikhmurzaev YD (1993) The moving contact line on a smooth solid surface. Int J Multi-Phase Flow 19:589–610

Van Mourik S, Veldman AEP, Dreyer ME (2005) Simulation of capillary flow with a dynamic contact angle. J Microgravity Sci Technol 17:87–93

Wang KL, Jones TB (2005) Electrowetting dynamics of microfluidic actuation. Langmuir 21:4211–4217